

Metal incorporation and heat-pulse measurement in amorphous-hydrogenated-silicon quantum devices

M. Jafar and D. Haneman

School of Physics, University of New South Wales, P.O. Box 1, Kensington 2033, Australia

(Received 13 July 1993)

Amorphous-hydrogenated-silicon double Schottky switching diodes in which one contact is vanadium, formed to produce switching, can show discrete steps in the I - V characteristics in the ON state at resistances of $h/2ne^2$ where n is an integer. We present experimental data to show that the forming temperature of the device is in excess of 1100 K, which can allow diffusion. Auger-electron-spectroscopy depth profiling shows that the top electrode penetrates significantly into the film in the formed devices, as theorized previously to explain the quantum phenomena. An elemental compositional analysis of the diffused metal region is presented. Resistance plots at various temperatures are consistent with the matrix containing vanadium particles.

I. INTRODUCTION

Amorphous-hydrogenated-silicon (ASIL) memory structures composed of double Schottky barriers including a vanadium contact, formed to produce switching, have been shown to possess steplike features in the ON state in their current-voltage characteristic.¹ The occurrence of the steps is at resistances R corresponding to $h/2ne^2$ where h is Planck's constant, e is the electronic charge, and n is an integer. The apparent quantized resistance values were observed at 4 K and, with decreasing prominence, at temperatures up to 190 K.¹ In some devices this effect was also reported to occur at room temperature.² This extraordinary behavior could not be accounted for by the authors with theories of quantized point contacts³⁻⁵ or ballistic electron transport^{3,4,6} due to the relatively high temperatures at which the phenomena occur, and no quantitative explanation was offered. We recently reported measuring quantized values at room temperature, from similar but not identical devices, and provided evidence that the quantized effects were real.⁷ We also presented a theory based on quantum confinement in small conducting inclusions, and demonstrated that our data at room temperature and those from Hajto *et al.*¹ at 4 K were in good agreement with the theoretical predictions. The major assumption in developing the theory was that the top metal contact, which appears to have to be vanadium for the steps to occur, penetrates into the amorphous silicon and forms chains of quantum-sized conducting inclusions. In this paper, we present experimental data which show that the temperature which occurs during the essential preliminary forming treatment, when a high current pulse density is passed, is in excess of 1100 K. This is more than sufficient for diffusion to occur. Depth-profiling Auger-electron spectroscopy (AES) was used to study the "formed" as well as unformed devices and a profile of elemental atomic concentration with depth was obtained for the formed and unformed devices. Clear evidence for vanadium penetration was obtained. Energy dispersive x-ray (EDX) data presented previously had barely shown

the presence of vanadium in the filamentary region.⁸ Resistance measurements as a function of temperatures were made and the behavior is consistent with the presence of conducting inclusions occurring in the matrix.

II. EXPERIMENT

The a -Si:H was prepared from the gas phase by the rf glow discharge method in a system described previously,⁹ in which simple p - i - n solar cells of over 5% unoptimized efficiency could be produced. The intrinsic material showed a 10^5 ratio of photoconductivity (at 1 sun) to dark conductivity and the hydrogen content, measured by elastic recoil detection, was around 18%.¹⁰

The devices used in this work were Cr- p^+ -V and Cr- p^+ -Ag. The p^+ layers were 200–400 nm thick, made using a discharge in silane with 10^4 V ppm of diborane on a substrate at 260°C, giving films with resistivity of $1.6 \times 10^4 \Omega \text{ cm}$. The top and bottom electrodes were deposited by vacuum evaporation. Devices with a top contact diameter of 70–100 μm were prepared as described previously.⁷

AES measurements were performed in a Kratos Surface Analysis System, XSAM 800. AES depth profiles were carried out on Cr- p^+ -V devices which were first formed by applying a 10–15-V pulse (vanadium positive), to produce switching properties, and which showed steps in the I - V ON characteristic. As a control, unformed devices were also analyzed. Scanning Auger microscopy (SAM) was used to center the electron beam onto the 70–100 μm V top electrode. A 5-kV argon ion beam, current 10 μA and argon pressure of 3×10^{-8} Torr, was rastered over an area of $(3 \times 3) \text{ mm}^2$ giving an etch rate of 162 $\text{\AA}/\text{min}$. (This rate was obtained in a separate calibration where the ion bombardment pit depth was measured with a profilometer.) The ratio of Auger-electron-beam diameter to raster area width was small, thus avoiding edge effects. The parameters for the Auger-electron beam were 5 kV and 15 nA.

Elemental atomic concentration was calculated using the area under the Auger peaks after background correction and using sensitivity factors for the various elements

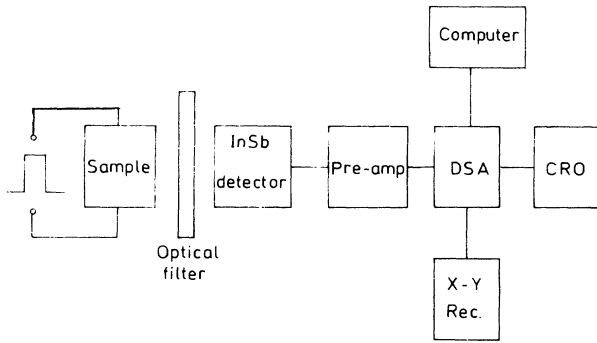


FIG. 1. Block diagram illustrating the arrangement used for thermal emission measurement during electrical pulsing. DSA is a digital storage adaptor.

as Si:0.30, V:0.37, Cr:0.30, C:0.15, O:0.40, and N:0.22.¹¹

Measurements of the temperature reached during forming were performed on unformed Cr- p^+ -Ag devices using the arrangement shown in Fig. 1. For the purpose of measuring temperatures, a 0.25-mm-thick sapphire substrate was used, so that the specimen could be observed through this from underneath. Observing radiation from the top was unsatisfactory as the top Ag contact blocked passage of infrared radiation. 20-ms pulses were applied to the sample, with the top (Ag) electrode positive. A liquid N₂ cooled InSb detector was placed within a few mm of the sample to measure the infrared heat signal resulting from electrical pulsing. Measurements over a range of wavelengths were taken using optical filters. The preamplifier had a gain of 10⁷ V/A. A digital storage adaptor (DSA) together with a computer, cathode ray oscilloscope (CRO), and x-y recorder were used to record the signals.

III. RESULTS

A typical emission signal received on the detector, without optical filtering, is shown in Fig. 2. In this case a

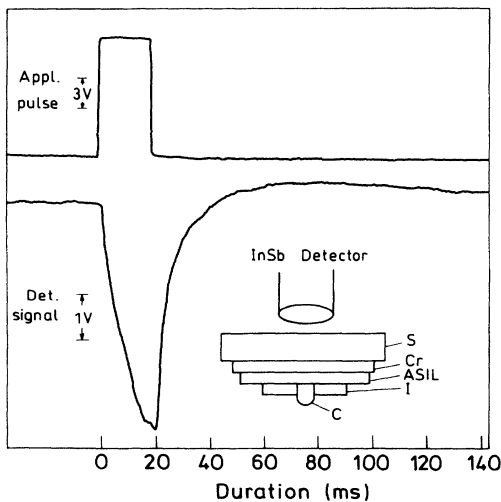


FIG. 2. Graphs showing the applied electrical pulse and the resulting thermal detector signal. The inset shows the configuration used. S is the sapphire substrate, Cr the chromium bottom electrode, I the insulator, and C the Ag top contact.

20-ms, 12.5-V square pulse was applied to an unformed Cr- p^+ -Ag device, with the Ag small-area contact positive. ac coupling was used for the input to the DSA to prevent any baseline shift. It was verified that this does not affect the rise or decay time of the signal. The inset in Fig. 2 shows the device structure, mounted on sapphire, and the position of the detector. It should be noted that the radiation signal rises rapidly for the duration of the pulse and then decays slowly. This is typical for thermal radiation. The decay time, depending on the pulse magnitude, was between 50 and 70 ms.

To determine the temperature, the radiation dispersion was measured using optical filters. Figure 3 shows data taken with the detector facing the top side (small-area contact) for a Cr- p^+ -Ag device on a glass substrate. The p^+ ASIL layer was 0.35 μm thick. In order to obtain a close estimate of the temperature attained during forming, voltage pulses (20 V) very close to the forming pulse (22–25 V) were applied. Making corrections for background, the peak intensity was found to be $\lambda_p = 3.63 \mu\text{m}$. From Wien's displacement law, $\lambda_p T = 2.8978 \times 10^{-3} \text{ mK}$, the forming temperature was derived as $T = 798 \text{ K}$. The blackbody curve at $T = 798 \text{ K}$ is drawn for comparison. This temperature, though quite appreciable, is not the true forming temperature. Note that the hottest spot would occur under the small-area silver contact, and with a comparatively large lump of silver sitting between the detector and the hot spot, the detector is only receiving radiation from the less hot boundary around the silver spot.

To obtain a better estimate of the true forming temperature a Cr- p^+ -Ag ($p^+ = 2800 \text{ \AA}$) device was fabricated on a 0.25-mm sapphire substrate. The infrared heat signal was measured in a similar way, but from the sapphire end, through the thin Cr film constituting the bottom contact. Figure 4 shows the data obtained for 20-ms pulses with magnitudes of 12.6 and 16 V. Note that the device "formed" when more measurements at 16 V were attempted. The radiation curve at 16 V, therefore, indicates a temperature which is very close to the true forming temperature of the device. Temperatures of 1017 K at 12.6 V (energy 3.7 μJ) and 1115 K at 16 V (6 μJ) were measured.

As a check on the reliability of the method, we mount-

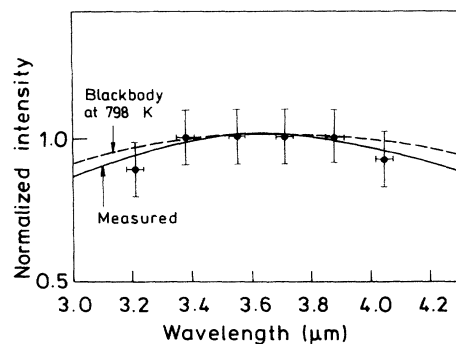


FIG. 3. Normalized heat intensity as a function of wavelength measured for radiation received from the top side of the device. The peak intensity is at $\lambda_p = 3.63 \mu\text{m}$.

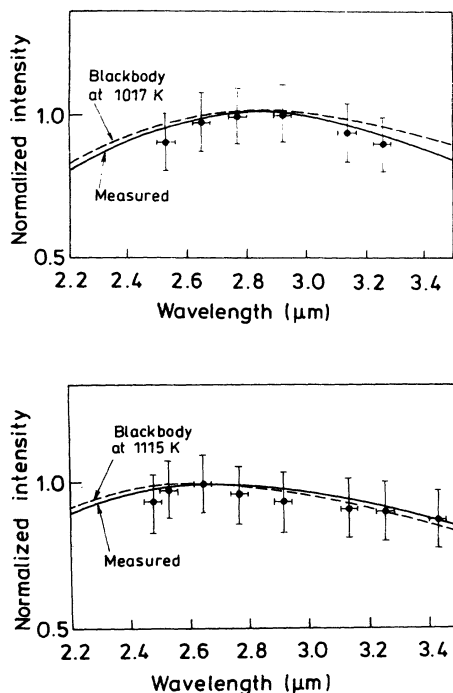


FIG. 4. (a) Normalized heat intensity as a function of wavelength, obtained with 12.6-V pulsing, showing the blackbody radiation peak at 2.85 μm . (b) Normalized heat intensity as a function of wavelength, obtained with 16-V pulsing, showing the blackbody radiation peak at 2.6 μm .

ed a quartz substrate coated with an ASIL film, inside a small coil furnace within a high vacuum system and under an optical window. A thermocouple was pressed against the bottom side of the substrate, and the temperature of the film on top was measured as before by detecting the thermal radiation with the cooled InSb detector and optical filters. This gave a temperature of 1070 K, whereas the thermocouple registered 1130 K. Considering that the thermocouple, from its location, might register a temperature slightly higher than that of the surface, the agreement is regarded as very good.

Attempts were made to detect radiation with a photomultiplier tube (PMT) (range, $\lambda < 0.68 \mu\text{m}$) instead of the InSb detector. However, no corresponding signal could be detected. This is not surprising since at about 1100 K, the radiation intensity at $\lambda = 0.6 \mu\text{m}$ is four orders of magnitude lower than at $\lambda_p = 2.6 \mu\text{m}$. The PMT did pick up a very weak contact junction electroluminescence signal characterized by much smaller rise and decay times of order μs . This emission is shown in Fig. 5.

The forming temperature of around 1100 K or more is very much higher than that estimated previously.¹² In the previous report a thin layer of liquid crystal, which undergoes a nematic-liquid phase transition at 35.3 $^{\circ}\text{C}$, was spread over the sample with a much smaller top contact. No observable temperature rise just prior to forming was detected by this method. It could, however, miss effects in very small times on very small areas. The authors had previously concluded that forming is an electronic process.¹³ The important parameters in both the

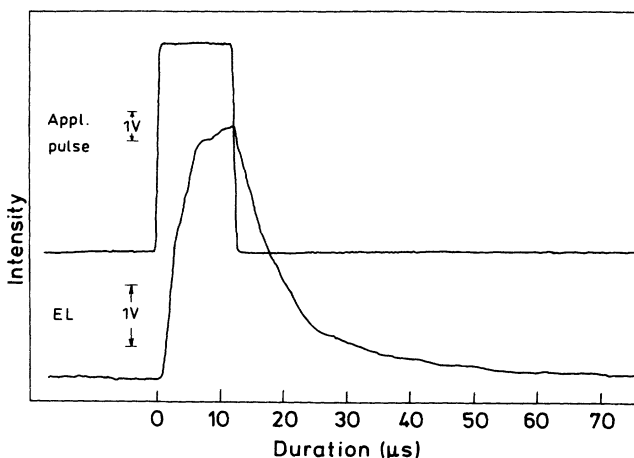


FIG. 5. Upper curve, applied voltage pulse. Lower curve, signal received from the photomultiplier, showing the contact junction electroluminescence emission.

previous work, using the quoted 1- μs pulses, and this work are given in Table I for comparison.

Both the energy density and the power density will affect the temperature rise, since the effects on heat generation of thermal conduction of surroundings are difficult to quantify. The densities quoted in the table are nominal, since the true areas of the conducting paths are less than those of the nominal top contact areas. Hence the differences in densities shown in the table may be misleading. If the power density is more critical, then the true forming temperature for smaller device areas would be even higher than the measured value in our case of greater than 1115 K. We believe that the occurrence of these high temperatures during the "forming" process enables the diffusion of contact material into the ASIL. Because the top contact of the device is so small compared with the bottom, the hottest spot is under the top contact and a temperature gradient exists between the top and the bottom. Thus it is material from the top contact that is involved. The reason why it is necessary to have a V top contact is presumably because this metal has the right properties for forming small droplets in the host matrix. Note that the diffusion of copper and aluminum in ASIL have been observed at temperatures as low as 150 $^{\circ}\text{C}$.¹⁴ The process of formation of inclusions is illustrated schematically in Fig. 6.

It is of interest to note that the ASIL material will lose hydrogen and decompose to microcrystalline silicon at the temperatures found to occur during forming. The degree to which this process takes place depends on the

TABLE I. Comparison of forming parameters.

	Hajto <i>et al.</i> (Ref. 6)	This work
Forming energy (J)	10^{-9}	6×10^{-6}
Device area (cm^2)	10^{-6}	8×10^{-5}
Nominal energy density (J/cm^2)	10^{-3}	8×10^{-2}
Nominal power density (W/cm^2)	1125	4

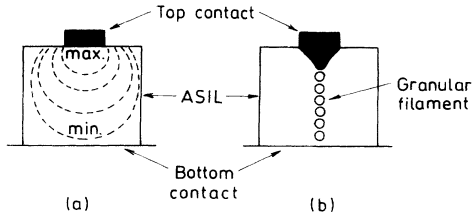


FIG. 6. Schematic diagram of (a) temperature gradient during forming and (b) the resulting granular filament due to top metal penetration into the ASIL layer.

time for which the material is sufficiently hot. This is a little longer than the time of the forming pulse, 20 ms in our case. It is possible that the formation of microcrystalline Si is involved in accounting for the switching behavior that is observed in formed devices. At present there is no satisfactory explanation of such behavior.

We show in Fig. 7 a scanning electron microscope picture of a vanadium contact as produced by evaporation through a rough hole in an insulating mask. Its dimensions are 60–70 μm . Figure 8 shows the depth-profiling AES spectra for an unformed and a formed Cr- p^+ -V device. The scan numbers on the traces correspond to measurements taken at different depths starting from the vanadium top electrode. Auger peaks for the various elements, in eV, can be seen at 92 (Si); 431, 473 (V); 487, 527, 571 (Cr); 271 (C); 383 (N); and 512 (O). Figure 8(a) for the formed Cr- p^+ -V device shows the depth profile over the three layers of the device: vanadium top contact (scans 1 and 2), ASIL layer (scans 3–13), and chromium bottom contact (scan 14). The spectra clearly show a mixing of vanadium and silicon over scans 3–8, whereas in a previous report⁸ EDX data had barely shown the present of vanadium in the filamentary region. The diminishing prominence of the vanadium peaks gives a perspective of the penetration pattern. Vanadium not being detected after scan 8 does not necessarily mean there is

no penetration beyond this depth. It only indicates that the concentration of vanadium is below the detectivity limit. (It is also possible that the diffused material is then off the line of the AES probe.) The region between scan 8 and 13 is believed to be responsible for producing the quantum jumps in the I - V characteristics,⁷ as this could contain the small particles of V previously hypothesized to exist,⁷ suspended in the matrix in the correct size and concentration.

As a control the AES measurements were also performed on an unformed device. The results for this are shown in Fig. 8(b). This again clearly shows the three layers of the device, however, no penetration of the top electrode was observed.

The percentage atomic concentrations were computed using the method outlined above. They are shown as functions of depth for a formed device (Fig. 9) and an unformed device (Fig. 10). The total vanadium and chromium concentrations are calculated by adding the concentrations of individual peaks. The depth is taken to be zero at the vanadium-silicon interface. In Fig. 9 a slight increase in concentration for some peaks at the beginning of the profile is attributed to improved surface texture after a few etches and a slightly decrease in concentration results when the profile reaches the glass substrate. Figure 9 shows that in the formed device the vanadium, together with oxygen and nitrogen, penetrates to a depth of at least 480 \AA . The true penetration depth is probably greater due to reasons outlined above. About 5–10% carbon seems to be present across the whole filament. Comparing the profiles in Figs. 9 and 10 at the silicon-chromium interface, there seems to be no major difference, confirming that the effects are due to the top contact. The profiles show a higher concentration of oxygen and carbon in the formed device. This is not surprising since the ASIL is exposed to air before evaporating the top contact. Hence carbon and oxygen contamination are present under the V, and would diffuse during forming.

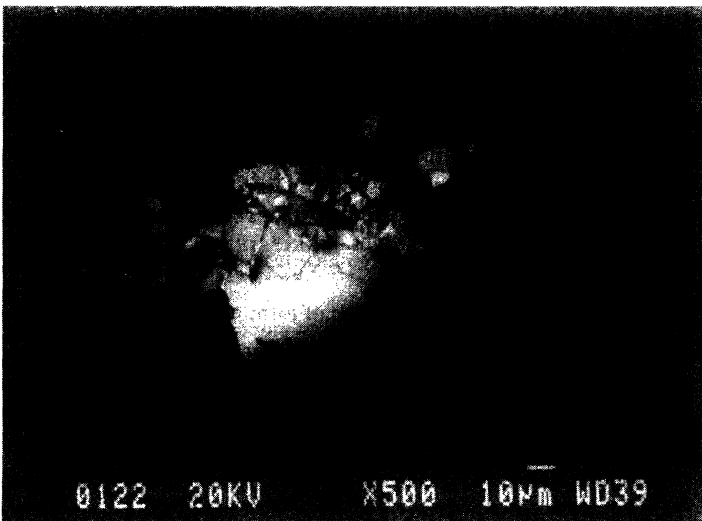


FIG. 7. Scanning electron micrograph of vanadium top contact on ASIL film. The two black spots are artifacts.

The high-temperature resistance R for granular structures in terms of activation energy E_a has been given as¹⁵

$$R = R_0 \exp(E_a / k_B T),$$

where k_B is the Boltzmann constant and T is the temperature. We tested this expression on $\text{Cr-p}^+\text{-V}$ devices in different resistance states. The resistance was measured as a function of temperature in the range from 296 to 400 K. The data for a typical sample are shown in Fig. 11. Note that the relation is obeyed, and that there appears to be a slight increase in the activation energy E_a in going from the low-resistance ON state (lower curves, $E_a \sim 0.02$ eV) to the high-resistance OFF state (upper curves, $E_a \sim 0.07$ eV). This is similar to the behavior found by Moser and Rohrer¹⁵ for granular filaments of metal formed in GaAs diodes. The phenomena are thus

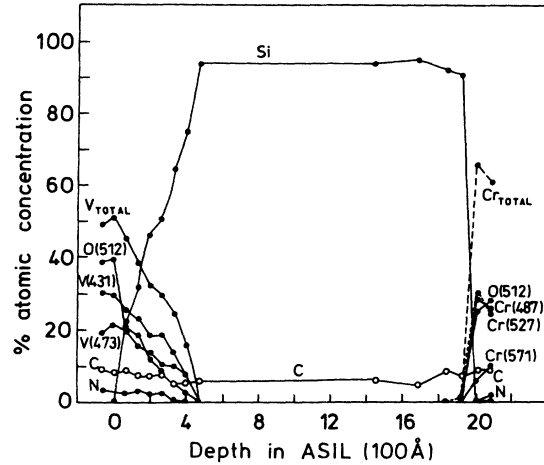


FIG. 9. Atomic concentration as a function of depth in $a\text{-Si:H}$ for a formed $\text{Cr-p}^+\text{-V}$ device, measured using AES.

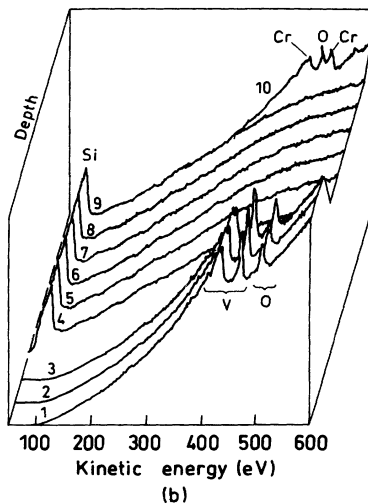
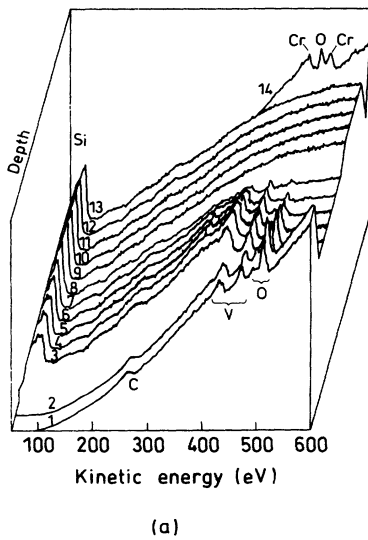


FIG. 8. AES depth profile on (a) a formed $\text{Cr-p}^+\text{-V}$ device clearly showing mixing of vanadium and silicon and (b) an unformed $\text{Cr-p}^+\text{-V}$ device verifying there is no mixing of vanadium and silicon prior to forming.

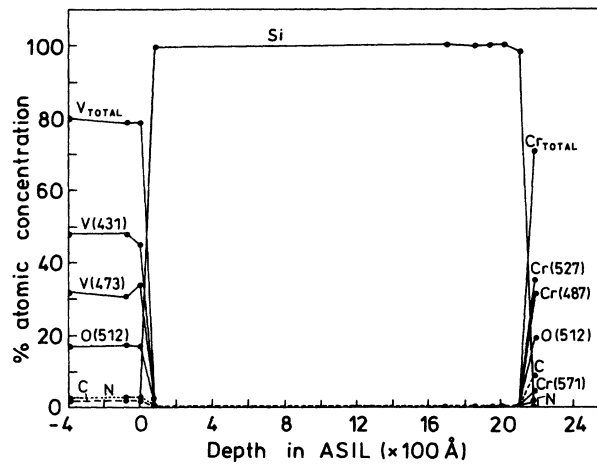


FIG. 10. Atomic concentration as a function of depth in $a\text{-Si:H}$ for an unformed $\text{Cr-p}^+\text{-V}$ device, measured using AES.

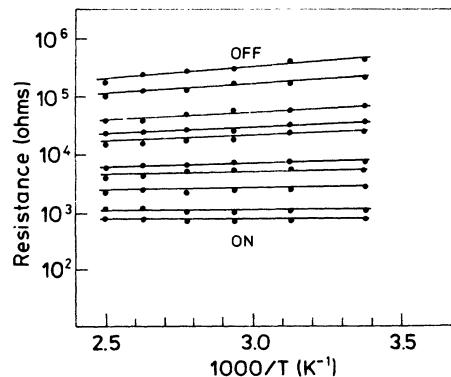


FIG. 11. Resistance as a function of $1/T$ for different memory states in a $\text{Cr-p}^+\text{-V}$ device.

consistent with our hypothesis of a granular filamentary structure.

IV. CONCLUSION

Our results show that the temperature reached in the devices during forming is in excess of 1100 K. This would cause the top contact to diffuse into the film. This has been verified using depth-profiling Auger-electron spectroscopy. Resistance plots as a function of tempera-

tures show behavior that is consistent with the presence of granular filaments.

ACKNOWLEDGMENTS

We are grateful for assistance with the thermal pulse measurements by Dr. N. S. McAlpine and D. G. Li. This work was supported by the Australian Research Council. M.J. thanks the Australian International Development Assistance Bureau for support.

-
- ¹J. Hajto, A. E. Owen, S. M. Gage, A. J. Snell, P. G. LeComber, and M. J. Rose, *Phys. Rev. Lett.* **66**, 1918 (1991).
²J. Hajto, M. J. Rose, A. J. Snell, I. S. Osborne, A. E. Owen, and P. G. LeComber, *J. Non-Cryst. Solids* **137&138**, 499 (1991).
³N. D. Lang, *Phys. Rev. B* **36**, 8173 (1987).
⁴A. Martin-Rodero, J. Ferrer, and F. Flores, *J. Microsc.* **152**, 317 (1988).
⁵J. K. Gimzewski and R. Moller, *Phys. Rev. B* **36**, 1284 (1987).
⁶J. Hajto, A. E. Owen, A. J. Snell, P. G. LeComber, and M. J. Rose, *Philos. Mag. B* **63**, 349 (1991).
⁷M. Jafar and D. Haneman, *Phys. Rev. B* **47**, 10911 (1993).
⁸M. J. Rose, J. Hajto, P. G. LeComber, A. J. Snell, A. E. Owen, and I. S. Osborne, in *Amorphous Silicon Technology-1991*, edited by A. Madan, Y. Hamakawa, M. J. Thompson, P. C. Taylor, and P. G. LeComber, MRS Symposia Proceedings

- No. 219 (Materials Research Society, Pittsburgh, 1991), p. 525.
⁹D. Haneman and D. H. Zhang, *Phys. Rev. B* **35**, 2536 (1987).
¹⁰A. Hoffman, D. D. Cohen, M. Jafar, and D. Haneman (unpublished).
¹¹L. E. Davies, N. C. MacDonald, P. W. Palmberg, G. E. Riach, and R. E. Weber, *Handbook of Auger Electron Spectroscopy* (Physical Electronics Industries, Inc., Minnesota, 1976), p. 14.
¹²P. G. LeComber, A. E. Owen, W. E. Spear, J. Hajto, A. J. Snell, W. K. Choi, M. J. Rose, and S. Reynolds, *J. Non-Cryst. Solids* **77&78**, 1373 (1985).
¹³A. E. Owen, P. G. LeComber, W. E. Spear, and J. Hajto, *J. Non-Cryst. Solids* **59&60**, 1273 (1983).
¹⁴S. Ishihara, *Thin Solid Films* **182**, 229 (1989).
¹⁵A. Moser and H. Rohrer, *Solid State Commun.* **17**, 939 (1975).



FIG. 7. Scanning electron micrograph of vanadium top contact on ASIL film. The two black spots are artifacts.